ACS APPLIED MATERIALS & INTERFACES



Article

# Self-Catalyzed Assembly of Peptide Scaffolded Nanozyme as a Dynamic Biosensing System

Hao Li, Yue Huang, Yue Yu, Genxi Li, and Yannis Karamanos

*ACS Appl. Mater. Interfaces*, **Just Accepted Manuscript** • DOI: 10.1021/acsami.5b11567 • Publication Date (Web): 11 Jan 2016



## Just Accepted



ACS Publications

ACS Applied Materials & Interfaces is published by the American Chemical Society.
1155 Sixteenth Street N.W., Washington, DC 20036

# Self-Catalyzed Assembly of Peptide Scaffolded Nanozyme as a Dynamic Biosensing System

Hao Li[†], Yue Huang[†], Yue Yu[‡], Genxi Li[†,§,*], Yannis Karamanos[//]

†. State Key Laboratory of Pharmaceutical Biotechnology and Collaborative Innovation Center of Chemistry for Life Sciences, Department of Biochemistry, Nanjing University, Nanjing 210093, China.

‡. Nanjing Drum Tower Hospital, The Affiliated Hospital of Nanjing University Medical School, Nanjing 210008, China.

§. Laboratory of Biosensing Technology, School of Life Sciences, Shanghai University, Shanghai 200444, China.

//. Laboratoire de la Barrière Hémato-encéphalique, Faculté des Sciences, Université d'Artois, rue Souvraz SP18, 62307 Lens Cedex, France.

Keywords： *Peptide self-assembly, Nanozyme, Amyloid-beta peptide, Catalytically self-propagating assembly, Peptide-based biosensing*

ABSTRACT：In this work, a new strategy of biosensor design is developed based on the assembly of amyloid beta and its multiple interactions with other bioactive species. These interactions can enable amyloid beta peptide as a multifunctional sensing element, so the immobilization of sensing probe and the step-by-step modification of the sensing interface have all been dispensed with. Instead, the kinetics of the assembly of a peptide-based catalytic network serves to convert the quantity of analyte into amplified signal readout. The designed dynamic assembling and biosensing system has also been successfully applied in detecting the activity of polyglutamylation, an essential post translation modification controlling cell skeleton and cell cycle, in biological complex samples. Further studies reveal that the serum abundance of a polyglutamylase, tubulin tyrosine ligase like protein 12, may show parallel with the degree of development of prostate cancer and the discrimination between early cancerous development and benign conditions. And the obtained result is more distinct than that based on PSA detection, the current gold standard. This study may also point to the prospective of extending this design strategy to broader range of biosensing applications in the future.

## INTRODUCTION

Over the last decade, biosensing systems have evolved from simple combination of probes[1-2] into sophisticated assemblage of nano- & bio-sensing elements[3-7], leading to major advances in analytical performance. However, the pace of this promising process has slowed down recently. It seems that the design of biosensing system has become a little too complicated, and the various components of the system may tend to cancel the beneficial effect of each other. This

points to a dilemma in biosensor design: while diversified sensing elements can produce powerful biosensing system, improper combination of these components may hamper the overall performance. Therefore it might be advantageous to come up with a novel overall layout as an alternative design of biosensing system.

Here a novel design is proposed (scheme 1) in which complexity of the biosensing system is balanced by dynamic interactions of the components. The inspiration comes from the biological systems[8-10], especially the cell signaling system, in which components engage in a dynamics of interactions, forming a network. Imitating this feature, the various components in the design proposed in this work can act in concert to achieve high performance. Meanwhile, the dynamics of components also enables one molecule, the amyloid beta peptide (A beta peptide), to play multiple biosensing roles[11-14].

A beta can bind with various molecular partners to acquire catalytic ability[15-19]. Taking advantage of these catalytic activities of A beta, a self-propagating route of A beta covalent assembly can be constructed (Scheme 1a). Cupric ion-complexed A beta can generate hydrogen peroxide under electrochemical agitation[13], while heme-complexed A beta can act as a peroxidase to expend the generated hydrogen peroxide[16] in the oxidation of tyrosine 10 on A beta[20], resulting in tyrosine bridged A beta cross-linking[21-22]. In this way, we can realize an electrochemically initiated and self-catalyzed assembly of an A beta-based nano-network containing great numbers of catalytic centers. This dynamic process of assembly can be integrated with the biosensing process by short peptide sequences capable of regulating the kinetics of A beta assembly. The pentameric peptide lysylleucylisoleucylphenylalanylphenylalanine (KLVFF) can prohibit the process of assembly[23], while the same sequence elongated by a polyglutamatic track controlling microtubule

cytoskeleton and cell fate[24-25], can function in the opposite way to accelerate the assembly[11] (Scheme 1b). So the presence of the track, as well as the activity of the relevant enzymes[26-27] can be probed by both the kinetics of assembly and the catalytic activity of the assembled network, since the catalytic route in the as-assembled network can be readily switched to catalyze the oxidative generation of electroactive reporter (Scheme 1c): electrochemically inactive o-phenylenediamine can be oxidatively cross-coupled to form electro-active 2,3-diaminophenazine[28]. In this design, the immobilization of sensing probe and the layer-by-layer modification of the sensing interface have all been dispensed with. Instead, the kinetics of the assembly of a peptide-based catalytic network serves to convert the quantity of analyte into amplified signal readout.

## EXPERIMENTAL SECTION

**Chemicals and Reagents** Peptide probe KLVFFE, polyglutamylated KLVFEEEEE were manufactured by Shanghai Science Peptide as lyophilized powder, purity>95%. Human recombinant tubulin tyrosine ligase like protein 12 was from Qrigene. Recombinant plasmin was provided by Milipore. Full length human amyloid-beta 1~42 (A beta) was from Sigma Aldrich. Analytical-grade was attained for all of the other reagents. Powder of the peptide probe was dissolved with 10 mM phosphate buffer solution (PBS) (pH 7.4) to the desired concentrations. A beta lyophilized powder was firstly dissolved in 1,1,1,3,3,3-hexafluoro-2-propa-nol (HFIP) at a concentration of 1 mg/mL to eliminate pre-existing aggregates. HFIP was subsequently evaporated under a gentle stream of high purity nitrogen, leaving behind a film that was later reconstituted with DMSO to 2.2 mM. This resuspension was further monomerized via sonication for 1 min, followed by being diluted to 440 μM with 10 mM PBS, pH 7.4, the above prepared solution of A beta was transparent without evident aggregation. This stock solution was kept at

4 °C for store and could be diluted to the desired concentrations with the same 10 mM PBS, pH 7.4, containing proper amount of $CuCl_2$ and Heme (originally dissolved with saturated NaOH to 10 mM). The original buffer solution of the target enzyme was dissolved with 10 mM PBS, pH 8.0, with 0.5 mM ATP, 2.4 mM $MgCl_2$. Redistilled water for preparation of all the solutions was prepared from distilled water with a Milli-Q purification system, the resistance of 18 MΩ·cm was achieved to guarantee the purity. The cell line MDA PCa, 22 Rv1 were purchased from ATCC and cultured following the instruction of the supplier in the supplier-provided medium. The cell line HEK 293T was kindly provided by the culture collection of the State Key Laboratory of Pharmaceutical Biotechnology of Nanjing University and cultured in Dulbecco's Modified Eagle Medium (Gibco co.) supplemented with 10% fetal calf serum (Hyclone co.) and maintained in a humidified atmosphere with 5% $CO_2$ at 37 °C. Serum samples of patients with prostate conditions were obtained from the Clinical Laboratory of the Nanjing Drum Tower Hospital, the Affiliated Hospital of Nanjing University Medical School, after elected consent by the local ethical committee.

**Electrode Treatment** Firstly, the gold disk electrode with a diameter of 3 mm was chemically cleaned for 5 min using Piranha rinsing solution, which was formulated by 70% sulfuric acid (concentrated) and 30% hydro-peroxide, followed with rinsing by double-distilled water. Then, the electrode was polished with fine sand paper, 1 μm and 0.3 μm alumina slurry in sequence, till achieving a mirror-smooth surface. Subsequently, water bath ultra-sonicating using both ethanol and water as the media was conducted to remove alumina powder from the electrode. Again, chemical cleaning was employed to clean the electrode: 50% nitric acid was incubated with the electrode for 30 min. Finally, electrochemical cleaning via repeated cyclic voltammetric scans in 0.5 M $H_2SO_4$ was utilized to remove any remaining impurities.

**Enzyme Activity Assay** Standard, spiked serum samples or original serum samples containing the target enzyme were 100× diluted sequentially with the solutions of the peptide probe and A beta, to desired concentrations of probe and A beta. The mixture was kept at 30 °C for proper time for the enzyme catalyzed polyglutamylation to proceed. Then the above cleaned electrode was immersed in the reaction mixture, and cyclic voltammetric scans with proper scanning parameters were applied to induce and regulate the assembly of A beta. Then, after gentle rinsing with dd$H_2O$ and PBS buffer, the electrode was ready for measurement. To generate readout signal, the electrode was transferred into 4 mL 10 mM PBS pH 7.4 containing 0.1 mg/ml o-phenylenediamine (OPD). Cyclic voltammetric scans similar to the above were applied and the solution gradually turned into yellow with a slight orange hue. Signal response of the generated 2,3-diaminophenazine (DPA) was then recorded.

**Experimental Measurements.** AFM images are recorded using ex situ Agilent 5500 AFM system. Samples were imaged at a scan rate of 0.5-1 Hz in a tapping mode. AFM tips with resonant frequency in a range 160-260 kHz were used. Images were acquired at a resolution of 512×512 pixels. Briefly, isothermal titration calorimetry (ITC) measurements were conducted using a MicroCal ITC200 System (GE healthcare life sciences). The titration was conducted at 25 °C. The titration schedule consisted of 38 consecutive injections of 1 μL with at least a 120 s interval between injections. Heats of dilution, measured by titrating beyond saturation, were subtracted from each data set. All solutions were degassed prior to titration. The data were analyzed using Origin 7.0 software. Electrochemical measurements were carried out on a CHI660D Potentiostat (CH Instruments) with a conventional three-electrode system: the electrode immobilized with peptide as the working electrode, a saturated calomel electrode (SCE) as the reference electrode and a platinum wire as the counter electrode. Square wave

voltammograms (SWVs) were recorded in 10 mM PBS, pH 7.4, which was deoxygenated by purging with nitrogen gas and maintained under this inert atmosphere during the electrochemical measurements.

## RESULT AND DISCUSSION

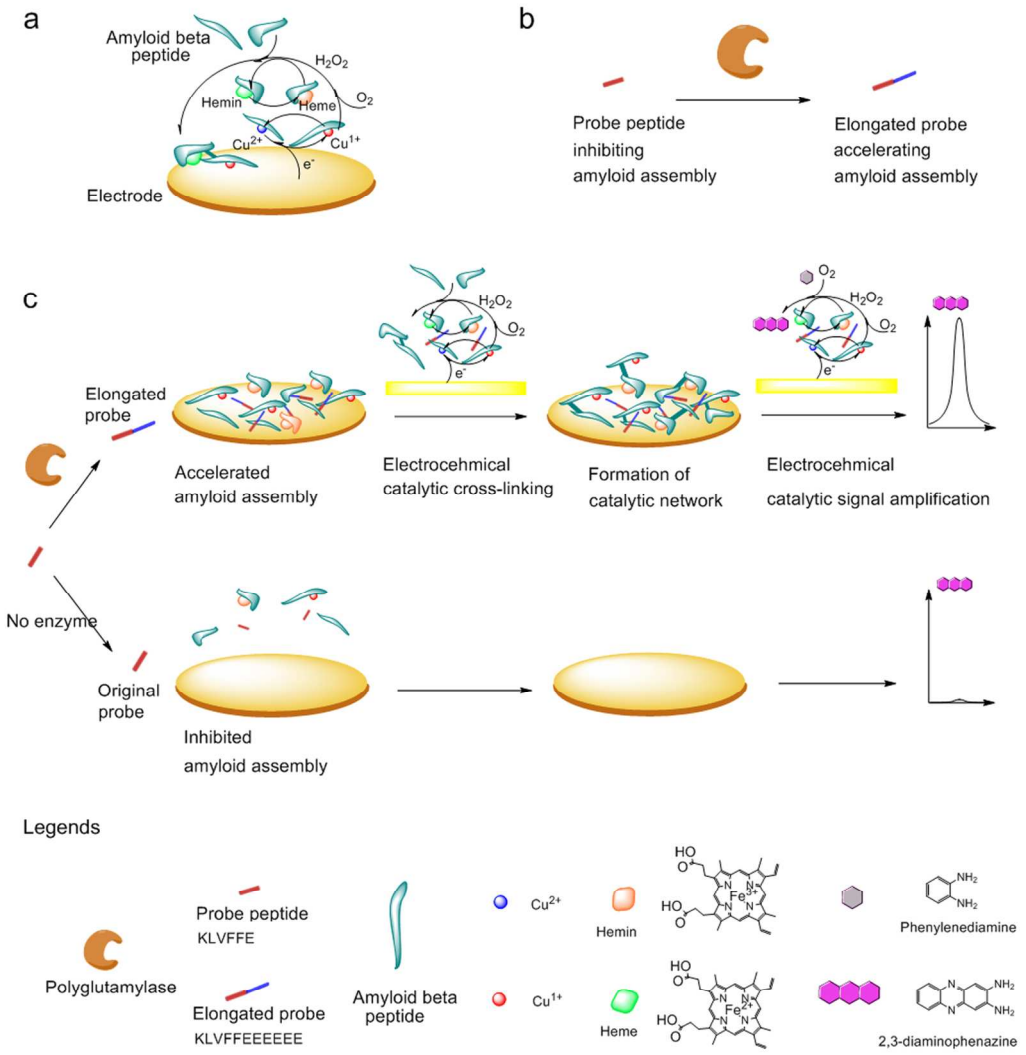


**Scheme 1.** Principle of the proposed dynamic assembling and biosensing system. (a) The proposed mechanism of electrochemically initiated covalent cross-linking and assembly of A beta, (b) the target enzyme catalyzes the elongation of the original probe to reverse its function. (c) Detection of polyglutamylase activity using the designed biosensing system.

The procedure of detection is illustrated in Scheme 1c. Polyglutamylase may turn the inhibitor peptide into accelerator sequence, and this sequence tends to attract molecules of A beta to the

proximity of each other. So, under proper electrochemical activation, the cupric ion- and heme-complexed A beta molecules, located rather close to each other, can form an effective catalytic route to cross-link the adjacent A beta molecules to form the network. On the contrary, in the absence of enzymatic activity, the ligand-complexed A beta molecules are so far away from each other, and prohibited from binding with each other by the inhibitor peptide, thus they cannot form the catalytic clusters required for cross-linking. Consequently, the network cannot growth out in short time. Therefore, in the former case, the network thus-formed on the electrode surface will contain a great number of catalytic clusters, capable of catalyzing the oxidative generation of a great many electroactive reporters. Nevertheless, in the latter case, hardly any reporter can be catalytically generated from the electrode surface sparsely populated by very little amount of A beta.

To realize the above design, the interactions of A beta with cupric ion and heme is first studied, using isothermal titration calorimetry (ITC). As can be observed in Figure S1~3, A beta shows moderate affinity[29-30] towards both species in their respective thermal titration experiments (Figure S1a,b), while the two types of interactions are comparable in strength. As is shown in Figure S2, both Cu (II) ion and heme fail to displace the other from A beta, when most A beta molecule are occupied. So, the two complexes formed respectively by cupric ion or heme with A beta can coexist in one system, as confirmed by the control experiments shown in Figure S3, where surplus A beta in the system of A beta complexed with one type of ligand can be occupied by the other ligand.

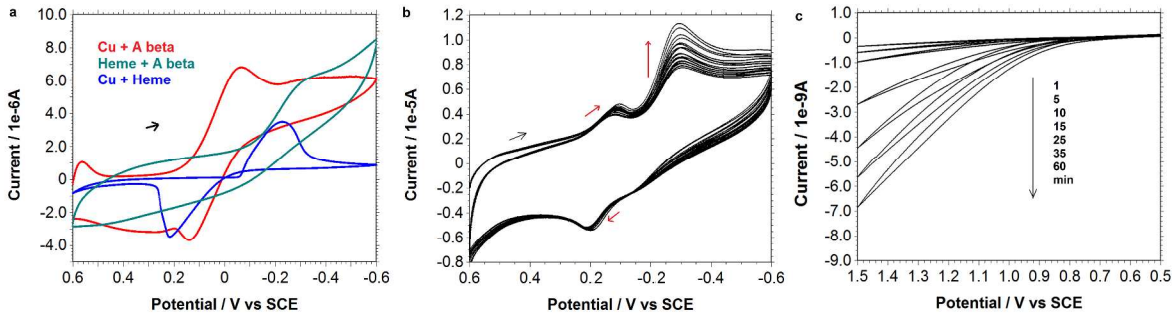


**Figure 1.** Validation of the electroactivity of the A beta-Cu(II) and A beta-heme complexes coexisted in the designed system. The data is recorded using a glassy carbon electrode, with 10 mM PBS (pH 7.4) as the supporting electrolyte. (a) Control experiments showing the red-ox activity of the components of the coexisted complexes, scan rate 0.1 V/s, the arrow marks scan direction. (b) Recorded electrochemical evolution of the designed system of coexisted complexes, scan rate 0.1 V/s, the black arrow marks scan direction, and the red arrows indicate the gradual changes in height and position of peaks. (c) Generation of peroxide recorded after electrochemical agitation of different duration.

These coexisted complexes form the basis of our design of the biosensing system, and their catalytic activity is designed to be electrochemically controllable to initiate peptide assembly and signal conversion. So, the electrochemical aspects of the formation and functioning of the complexes are subsequently studied. First, the formation of the complexes is further confirmed by their electrochemical behavior in a series of control experiments (Figure 1a). As shown by the blue curve, a system of heme and $Cu^{2+}$ but without A beta gives the reduction peak of heme (Hemin/Heme -0.15 V vs SCE, as a shoulder peak of the anodic peak of copper in Figure 1a, separately shown in Figure S4a)[12] and the peaks of copper (reduction: $Cu^{2+}$/Cu -0.2 vs SCE, oxidation: $Cu^{2+}$/Cu 0.2 vs SCE, Figure S4b)[31]. On the contrary, quasi-reversible reduction-oxidation peak pairs around 0.08 V vs SCE are observed in a cupric ion-A beta system (red

curve), indicating prevention of reduction to $Cu^0$ through formation of complex. Meanwhile, in the heme-A beta system, negatively shifted reduction peak is observed (teal curve), suggesting the formation of heme-A beta complex. These results are also consistent with previous reports on the formation of Cu (II)-A beta[13] and Heme-A beta[12] complexes. Figure 1b shows that, if coexisted, these two complexes show their respective peaks (Figure 1b) similar to those observed separately in Figure 1a (red and teal curves). Further, proper electrochemical agitation may be able to reduce the metal ion contained in the complexes to initiate Fenton-like reactions[19] in generating and consuming peroxide. This process of electrochemical evolution can be observed in Figure 1b, where the presence of gradually increased reduction peak of both heme and cupric ion might be ascribed to the more and more metal species being gradually electrochemically regenerated after catalyzing reactions of peroxide generation and peroxidation. This last point can be confirmed directly by the electrochemical response of peroxide generated by the above process (Figure 1c), with larger response observed from electrochemical treatment lasting longer.

The effect of the above electrochemical catalysis lies in the oxidative formation of di-tyrosine to covalently cross-link and assemble A beta. This cross-linking mechanism has been proposed for A beta associated pathology in various previous reports[14, 21-22], but this is the first time that it is employed to build a biosensing system. As previously described, for biosensing purpose, a regulatory peptide of A beta assembly is employed at the same time as the probe, and activity of the target enzyme can elongate this probe sequence to reverse its effect of retarding A beta assembly. So here the effect of the probe in regulating the electrochemically facilitated A beta assembly is investigated. Firstly, the kinetics of A beta assembly regulated by the original and the elongated peptide is followed electrochemically via the oxidative response of tyrosine 10 of A beta (Figure S5, S6). Contrasting the two sets of results, two points become evident, first, the

opposite effect of the two probes are sufficient to enable biosensing application; second, in the fast kinetics triggered by the elongated probe, more di-tyrosine has been formed[32]. Since this cross-linker cannot subsequently be properly oxidized electrochemically[33], decreased overall response of tyrosine is observed. The result may validate the molecular proximity of A beta induced by the elongated probe, and this mechanism has greatly accelerated assembly process by enhancing the cross-linking of A beta. Besides, the structural feature of the assembled network has also been studied by conformation-directed dye thioflavin T which is known to target beta sheet in A beta[34]. As can be discovered by comparing Figure S7, S8, besides the dramatic difference in kinetics similar to that evidenced by tyrosine 10 of A beta, thioflavin T response[35] also drops in the case of the elongated probe, again indicating cross-linking induced fast assembly. Atomic force microscopic morphology of the network also confirms the electrochemically detected difference in kinetics and mechanism of assembly (Figure S9). The bi-functional role of A beta in the biosensing system can be confirmed with control experiments (Figure S10) which show that the assembly of A beta can serve to convert activity of the target enzyme into signal readout, while the subsequent formation of A beta-based nanoenzyme can act to amplify the signal. Meanwhile, the signal amplification induced by coexist of cupric ion and hemin has also been verified by control experiments (Figure S11), in which the signal responses of Cu (II)-A beta or Heme-A beta alone are much smaller than that of the coexisted system.

The above results have validated the proposed design of electrochemically facilitated and self-catalyzed assembly of A beta the kinetics of which can also be regulated by the biosensing probe. The assembled network contains large numbers of active centers that is employed to catalyze oxidative generation of the final signal reporter. Using the response of this reporter, various aspects of the biosensor have been investigated for improved analytical performance. First, the

concentration of A beta for assembling is optimized (Figure S12). Higher A beta concentration admits greater amount of catalytic centers to be incorporated in the assembled network, but at the same while this dense network also hampers the interface electron transfer, leading to decreased final signal readout. As can be figured out from Figure S12, a balanced concentration of A beta can be found around 30 μM. The same principle applies for the concentration of the probe, and at about 10 μM, the probe-A beta system can give rise to a not too dense network with a large number of catalytic centers of prominent signal readout (Figure S13). Next, concentrations of the catalytic-active species are studied. Cupric ion is responsible for generating peroxide, initially the final signal increases with the concentration of cupric ion (Figure S14), but surplus cupric ion can form complex with A beta at greater than 1:1 molecular ratio, leading to directly cupric ion-catalyzed A beta cross-linking. The dense network thus formed offsets the effect of the greater number of catalytic centers retained on the electrode surface, so the balanced cupric ion is selected around 10 μM. On the other hand, heme, as the cofactor for peroxidase-like activity of the assembled A beta network, approaches saturation of the catalytic effect at around 10 μM (Figure S15). Consequently, the optimal molecular ratio of cupric ion to heme is found around 1:1 (Figure S16). Finally, electrochemical parameters controlling the process of A beta assembly are optimized, such as the duration and potential range of cyclic voltammetric scanning (Figure S17, S18). Based on these results, moderate electrochemical treatments are adopted to avoid excessive network formation to foul the electrode surface. The stability of the assembled nanozyme has also been verified by control experiments (Figure S19), in which the drop of signal readout is acceptable after several hours to several days of store.

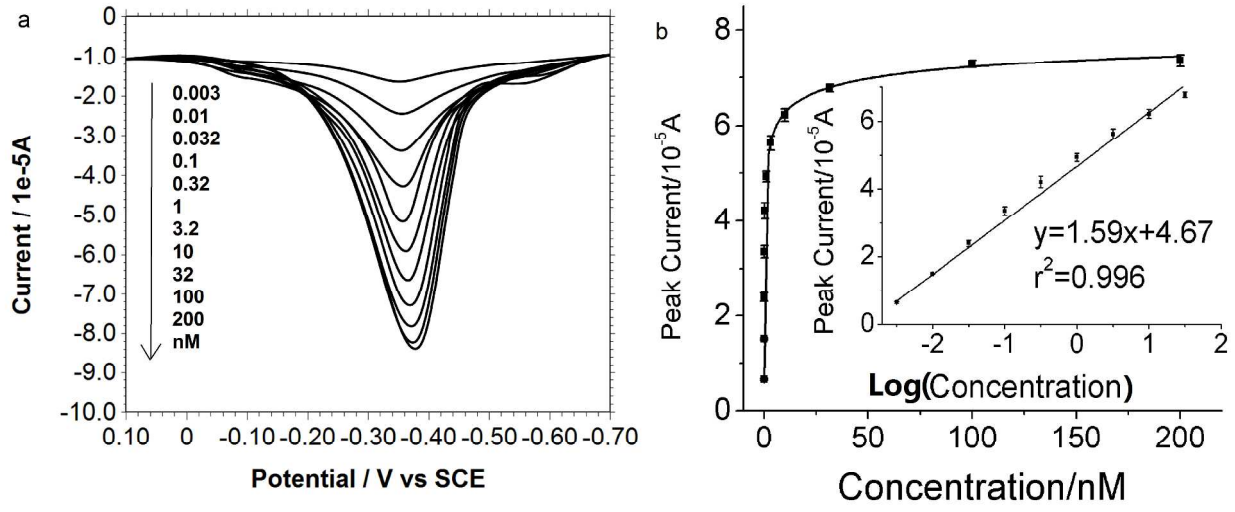


**Figure 2.** Quantitative analysis of tubulin tyrosine ligase like protein 12 (TTLL12) using the proposed dynamic assembling and biosensing system. The target enzyme first catalyzes elongation of the probe in the presence of the co-existed A beta, heme and Cu ion, the working electrode is then immerged in this solution for the electrochemically controlled formation of the catalytic network on the electrode surface, followed by being transferred into the solution of OPD to catalyze its oxidation, and the electrochemical response of the product DAP is then recorded. (a) Square wave voltammograms (SWVs) of 2,3-diaminophenazine (DPA) showing the gradual increase of signal response with the abundance of active TTLL12. (b) Peak currents in (a) plotted as a function of TTLL12 concentration. Inset is the linear range and the corresponding formula obtained via regression analysis. The error bars represent standard deviation from average (n=3).

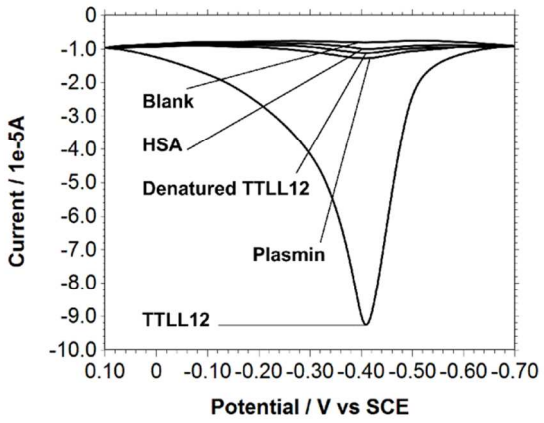


**Figure 3.** SWVs of DAP showing the specificity of the assay. All control species are of 10 nM, while human albumin (HSA) is of excessive amount. The data is obtained following the same procedure as described in Figure 2.

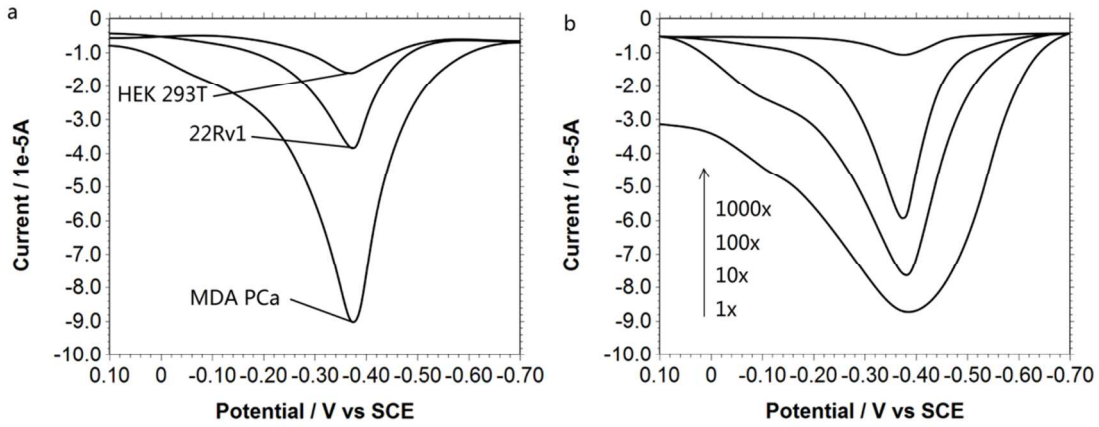


**Figure 4.** SWVs obtained in detecting biological samples. The data is obtained following the same procedure as described in Figure 2. (a) The signal responses of fractioned cell samples (around $1\times10^6$ cell/mL). (b) The responses in detecting spiked serum samples, the 1× sample is prepared by diluting recombinant TTLL12 with the serum of healthy volunteer to 10 nM, and then serially diluted as indicated on the figure.

Under these optimized conditions, the polyglutamylase responsible for elongation of the probe

can be detected with the designed dynamic assembling and biosensing system. First, the time course of the target enzyme interacting with the A beta-probe system is studied (Figure S20) and saturation can be approached within 60 min of interaction. Proportional increase in signal readout is achieved in detecting the activity of polyglutamylase, and a linear range between signal readout and the logarithm of the amount of active enzyme can be established from 3 pM to 30 nM (Figure 2). The standard deviation in all repetitive measurements is within 5%, showing a good reproducibility. The biosensing system is then interrogated with a series of control species, including major serum proteins such as albumin and plasmin, no evident interference is observed, suggesting a satisfactory specificity of the design (Figure 3). This specificity can be contributed to the fact that only the activity of the target enzyme can elongate the probe to induce A-beta assembly and the formation of the catalytic network, while the other proteins have no such activity. In the detection of 100× diluted cell samples, polyglutamylase activity is found in parallel with the degree of malignancy (Figure 4a). The highest activity is related, by the assay with the proposed method, to metastasis-derived cell line; the immortalized normal cell line shows the lowest activity; while the intermediate level of activity is found in the cell line raised through passage in mice as xenograph. To apply the proposed method in detecting serum samples, the extent of interference is studied in spiked serum samples prepared with different folds of dilution (Figure 4b). The undiluted sample gives rise to a very broad peak with relatively high background as well as the signs of shoulder peak, these effects of interference are gradually suppressed by more extensive dilution, and 100× dilution may yield balanced signal readout with no evident interference and relatively large response. These results have preliminarily proved the feasibility of the proposed method in detecting diluted biological samples, so it can be extended to clinical samples.

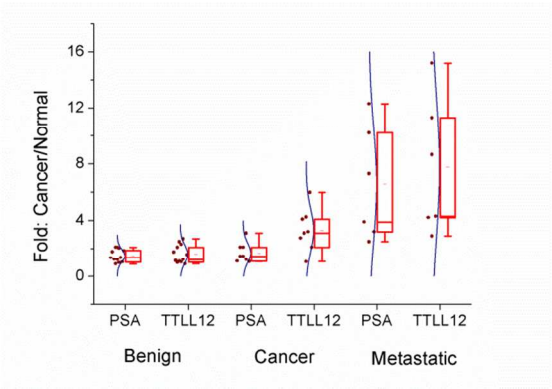


**Figure 5.** Box chart to show the distribution of the detected level of PSA, and the activity of TTLL12 in patients with prostate conditions, grouped by degree of disease development. The level of PSA is assayed with an ELISA kit commercially available, and the activity of TTLL12 is detected using the proposed method. For each sample, the detected biomarker abundance and activity in pathological condition is normalized as the fold of increase compared with that of healthy volunteers. The raw data is included as a column scatter plot to the left of each box. A curve corresponding to normal distribution is also displayed on top of the scatter plot.

The target polyglutamylase, tubulin tyrosine ligase like protein 12 (TTLL12), controls the architectural features of microtubule cytoskeleton of cell by tubulin polyglutamylation. TTLL12 is constitutionally up-regulated in neurons to maintain the dynamic balance of microtube-supported dendrites, and recently TTLL-dependent neurotoxic mechanism has been discovered for A beta[36]. On the other hand, microtube also forms the cellular machinery for mitosis, so severing of microtube by TTLL activity is potentially related to the disrupted cell cycle essential to neuplastic developments. In light of these previous results, clinical serum samples of patients with benign or cancerous conditions are detected for TTLL12 activity (Figure 5). The parallel between detected activity and the progress of disease is evident, while the level of the current gold standard PSA, assayed with commercially available ELISA kit, shows similar trend, but the

discrimination between benign and cancerous condition is not that evident compared with TTLL12, so TTLL12, examined by our method, is a more promising biomarker in prostate cancer. Previous reports based on classical biochemical methodology also support this result[37-38].

## CONCLUSIONS

In this work, the assembly of amyloid beta and its interactions with various other bioactive species are employed to develop a novel biosensing strategy. This method employs the kinetics of the assembly of a peptide-based catalytic network to convert the quantity of analyte into amplified signal readout. The immobilization of probe, and the step-by-step modification and treatment of the sensing interface have all been dispensed with. The designed dynamic assembling and biosensing system has been successfully applied in detecting the activity of polyglutamylation, an essential post translation modification controlling cell skeleton and cell cycle, in biological complex samples. This favorable performance may enable prospective applications of the proposed method in clinical bioanalysis in the future.

## ASSOCIATED CONTENT

**Supporting Information**. Validation of the principle of design and optimization of various experimental conditions. The supporting material is available free of charge via the Internet at http://pubs.acs.org."

## AUTHOR INFORMATION

### Corresponding Author

*Corresponding author at Department of Biochemistry, Nanjing University, Nanjing 210093, China. Fax: +86 25 83592510. E-mail address: genxili@nju.edu.cn.

## ACKNOWLEDGMENT

This work is supported by the National Natural Science Foundation of China (Grant Nos. 21235003, 81501554, J1103512, J1210026).

## REFERENCES

1. Chaubey, A.; Malhotra, B. D., Mediated biosensors. *Biosen.Bioelectron.* **2002,** *17*, 441-456.
2. Zhang, S.; Wright, G.; Yang, Y., Materials and techniques for electrochemical biosensor design and construction. *Biosen. Bioelectron.* **2000,** *15*, 273-282.
3. Ambrosi, A.; Chua, C. K.; Bonanni, A.; Pumera, M., Electrochemistry of Graphene and Related Materials. *Chem. Rev.* **2014,** *114*, 7150-7188.
4. Gui, G.; Zhuo, Y.; Chai, Y.-Q.; Liao, N.; Zhao, M.; Han, J.; Zhu, Q.; Yuan, R.; Xiang, Y., Supersandwich-type electrochemiluminescenct aptasensor based on Ru(phen)(3)(2+) functionalized hollow gold nanoparticles as signal-amplifying tags. *Biosen. Bioelectron.* **2013,** *47*, 524-529.
5. Lung Khung, Y.; Narducci, D., Synergizing nucleic acid aptamers with 1-dimensional nanostructures as label-free field-effect transistor biosensors. *Biosens. Bioelectron.* **2013,** *50*, 278-93.
6. Saha, K.; Agasti, S. S.; Kim, C.; Li, X.; Rotello, V. M., Gold Nanoparticles in Chemical and Biological Sensing. *Chem. Rev.* **2012,** *112*, 2739-2779.
7. Yan, J.; Hu, C.; Wang, P.; Zhao, B.; Ouyang, X.; Zhou, J.; Liu, R.; He, D.; Fan, C.; Song, S., Growth and Origami Folding of DNA on Nanoparticles for High-Efficiency Molecular Transport in Cellular Imaging and Drug Delivery. *Angew. Chem. Inter. Ed.* **2015,** *54*., 2431-2435.

8. Androulakis, I. P.; Kamisoglu, K.; Mattick, J. S., Topology and Dynamics of Signaling Networks: In Search of Transcriptional Control of the Inflammatory Response. *Annu. Rev. Biomed. Eng., Vol 15* **2013,** *15*, 1-28.

9. Garcia-Garcia, J.; Bonet, J.; Guney, E.; Fornes, O.; Planas, J.; Oliva, B., Networks of Protein-Protein Interactions: From Uncertainty to Molecular Details. *Mol. Inf.* **2012,** *31*, 342-362.

10. Riccione, K. A.; Smith, R. P.; Lee, A. J.; You, L., A Synthetic Biology Approach to Understanding Cellular Information Processing. *ACS Synth. Biol.* **2012,** *1*, 389-402.

11. Lowe, T. L.; Strzelec, A.; Kiessling, L. L.; Murphy, R. M., Structure-function relationships for inhibitors of beta-amyloid toxicity containing the recognition sequence KLVFF. *Biochemistry* **2001,** *40*, 7882-7889.

12. Zhou, Y.; Wang, J.; Liu, L.; Wang, R.; Lai, X.; Xu, M., Interaction between Amyloid-beta Peptide and Heme Probed by Electrochemistry and Atomic Force Microscopy. *ACS Chem. Neurosci.* **2013,** *4*, 535-539.

13. Jiang, D.; Men, L.; Wang, J.; Zhang, Y.; Chickenyen, S.; Wang, Y.; Zhou, F., Redox reactions of copper complexes formed with different beta-amyloid peptides and their neuropathalogical relevance. *Biochemistry* **2007,** *46*, 9270-9282.

14. Al-Hilaly, Y. K.; Williams, T. L.; Stewart-Parker, M.; Ford, L.; Skaria, E.; Cole, M.; Bucher, W. G.; Morris, K. L.; Sada, A. A.; Thorpe, J. R.; Serpell, L. C., A central role for dityrosine crosslinking of Amyloid-beta in Alzheimer's disease. *Acta Neuropathol. Commun.* **2013,** *1*, 83-83.

15. Pramanik, D.; Dey, S. G., Active Site Environment of Heme-Bound Amyloid beta Peptide Associated with Alzheimer's Disease. *J. Am. Chem. Soc.* **2011,** *133*, 81-87.

16. Pramanik, D.; Ghosh, C.; Mukherjee, S.; Dey, S. G., Interaction of amyloid beta peptides with redox active heme cofactor: Relevance to Alzheimer's disease. *Coordin. Chem. Rev.* **2013,** *257*, 81-92.

17. Smith, D. G.; Cappai, R.; Barnham, K. J., The redox chemistry of the Alzheimer's disease amyloid beta peptide. *Biochim. Biophys. Acta, Biomembr.* **2007,** *1768*, 1976-1990.

18. Lin, C.-J.; Huang, H.-C.; Jiang, Z.-F., Cu(II) interaction with amyloid-beta peptide: A review of neuroactive mechanisms in AD brains. *Brain Res. Bull.* **2010,** *82*, 235-242.

19. La Penna, G.; Hureau, C.; Andreussi, O.; Faller, P., Identifying, By First-Principles Simulations, Cu Amyloid-beta Species Making Fenton-Type Reactions in Alzheimer's Disease. *J. Phys. Chem. B* **2013,** *117*, 16455-16467.

20. Ali, F. E.; Barnham, K. J.; Barrow, C. J.; Separovic, F., Metal catalyzed oxidation of tyrosine residues by different oxidation systems of copper/hydrogen peroxide. *J. Inorg. Biochem.* **2004,** *98*., 173-184.

21. Atwood, C. S.; Perry, G.; Zeng, H.; Kato, Y.; Jones, W. D.; Ling, K. Q.; Huang, X. D.; Moir, R. D.; Wang, D. D.; Sayre, L. M.; Smith, M. A.; Chen, S. G.; Bush, A. I., Copper mediates dityrosine cross-linking of Alzheimer's amyloid-beta. *Biochemistry* **2004,** *43*, 560-568.

22. Smith, D. P.; Ciccotosto, G. D.; Tew, D. J.; Fodero-Tavoletti, M. T.; Johanssen, T.; Masters, C. L.; Barnham, K. J.; Cappai, R., Concentration dependent Cu2+ induced aggregation and dityrosine formation of the Alzheimer's disease amyloid-beta peptide. *Biochemistry* **2007,** *46*, 2881-2891.

23. Tjernberg, L. O.; Naslund, J.; Lindqvist, F.; Johansson, J.; Karlstrom, A. R.; Thyberg, J.; Terenius, L.; Nordstedt, C., Arrest of beta-amyloid fibril formation by a pentapeptide ligand. *J. Biol. Chem.* **1996,** *271*, 8545-8548.

24. Lacroix, B.; van Dijk, J.; Gold, N. D.; Guizetti, J.; Aldrian-Herrada, G.; Rogowski, K.; Gerlich, D. W.; Janke, C., Tubulin polyglutamylation stimulates spastin-mediated microtubule severing. *J. Cell Biol.* **2010,** *189*, 945-954.

25. van Dijk, J.; Rogowski, K.; Miro, J.; Lacroix, B.; Edde, B.; Janke, C., A targeted multienzyme mechanism for selective microtubule polyglutamylation. *Mol. Cell* **2007,** *26*, 437-448.

26. Kashiwaya, K.; Nakagawa, H.; Hosokawa, M.; Mochizuki, Y.; Ueda, K.; Piao, L. H.; Chung, S. Y.; Hamamoto, R.; Eguchi, H.; Ohigashi, H.; Ishikawa, O.; Janke, C.; Shinomura, Y.; Nakamura, Y., Involvement of the Tubulin Tyrosine Ligase-Like Family Member 4 Polyglutamylase in PELP1 Polyglutamylation and Chromatin Remodeling in Pancreatic Cancer Cells. *Cancer Res.* **2010,** *70*, 4024-4033.

27. Das, V.; Kanakkanthara, A.; Chan, A.; Miller, J. H., Potential role of tubulin tyrosine ligase-like enzymes in tumorigenesis and cancer cell resistance. *Cancer Lett.* **2014,** *350*, 1-4.

28. Song, J. F.; Zhao, M. R.; Guo, W.; Wang, J. X., Polarographic immunoassay coupled with catalytic amplification of labeled copper ions. *Sci. China, Ser. B-Chemistry* **1997,** *40*, 561-567.

29. Tougu, V.; Karafin, A.; Palumaa, P., Binding of zinc(II) and copper(II) to the full-length Alzheimer's amyloid-beta peptide. *J. Neurochem.* **2008,** *104*, 1249-1259.

30. Atamna, H.; Frey, W. H., II; Ko, N., Human and rodent amyloid-beta peptides differentially bind heme: Relevance to the human susceptibility to Alzheimer's disease. *Arch. Biochem. Biophys.* **2009,** *487*, 59-65.

31. Shin, H.; Park, M.; Kim, A. R.; Kang, C., Electrochemical measurements of Cu2+ ions adsorbed on an electrochemically oxidized glassy carbon electrode. *J. Electroanal. Chem.* **2003,** *547*, 143-149.

32. Jang, H.-S.; Lee, J.-H.; Park, Y.-S.; Kim, Y.-O.; Park, J.; Yang, T.-Y.; Jin, K.; Lee, J.; Park, S.; You, J. M.; Jeong, K.-W.; Shin, A.; Oh, I.-S.; Kwon, M.-K.; Kim, Y.-I.; Cho, H.-H.; Han, H. N.; Kim, Y.; Chang, Y. H.; Paik, S. R.; Nam, K. T.; Lee, Y.-S., Tyrosine-mediated two-dimensional peptide assembly and its role as a bio-inspired catalytic scaffold. *Nat. Commun.* **2014,** *5*.

33. Jacob, J. S.; Cistola, D. P.; Hsu, F. F.; Muzaffar, S.; Mueller, D. M.; Hazen, S. L.; Heinecke, J. W., Human phagocytes employ the myeloperoxidase-hydrogen peroxide system to synthesize dityrosine, trityrosine, pulcherosine, and isodityrosine by a tyrosyl radical-dependent pathway. *J. Biol. Chem.* **1996,** *271*, 19950-19956.

34. Biancalana, M.; Koide, S., Molecular mechanism of Thioflavin-T binding to amyloid fibrils. *Biochim. Biophys. Acta, Proteins Proteomics* **2010,** *1804*, 1405-1412.

35. Dounin, V.; Constantinof, A.; Schulze, H.; Bachmann, T. T.; Kerman, K., Electrochemical detection of interaction between Thioflavin T and acetylcholinesterase. *Analyst* **2011,** *136*, 1234-1238.

36. Zempel, H.; Luedtke, J.; Kumar, Y.; Biernat, J.; Dawson, H.; Mandelkow, E.; Mandelkow, E.-M., Amyloid-beta oligomers induce synaptic damage via Tau-dependent microtubule severing by TTLL6 and spastin. *Embo J.* **2013,** *32*, 2920-2937.

37. Massoner, P.; Lueking, A.; Goehler, H.; Hoepfner, A.; Kowald, A.; Kugler, K. G.; Amersdorfer, P.; Horninger, W.; Bartsch, G.; Schulz-Knappe, P.; Klocker, H., Serum-autoantibodies for discovery of prostate cancer specific biomarkers. *Prostate* **2012,** *72*, 427-436.

38. Wasylyk, C.; Zambrano, A.; Zhao, C.; Brants, J.; Abecassis, J.; Schalken, J. A.; Rogatsch, H.; Schaefer, G.; Pycha, A.; Klocker, H.; Wasylyk, B., Tubulin tyrosine ligase like 12 links to prostate cancer through tubulin posttranslational modification and chromosome ploidy. *Inter. J. Cancer* **2010,** *127*, 2542-2553.

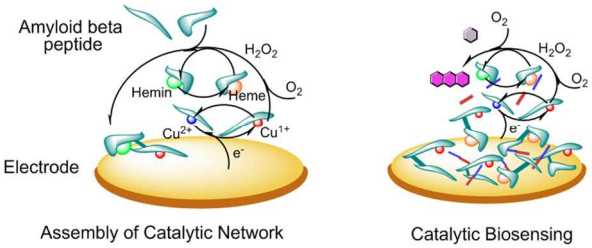


Table of Contents (TOC) graphic